Chemical Engineering & Processing: Process Intensification 183 (2023) 109257

Contents lists available at ScienceDirect

Chemical Engineering and Processing - Process Intensification

journal homepage: www.elsevier.com/locate/cep

Back extraction combined with magnetic solid phase extraction based on bubble column for separation and purification of juglone from *Juglans mandshurica* Maxim. coproducts

Mengfei Tian [a], Xianming Meng [a], Naveed Ahmad [b], Chunying Li [a], Zhanyu Yuan [c], Zidan Luo [a], Yu Zhang [a], Chunyu Liang [a], Chunjian Zhao [a,*]

[a] College of Chemistry, Chemical Engineering and Resource Utilization, Northeast Forestry University, Harbin 150040, China; Key Laboratory of Forest Plant Ecology, Ministry of Education, Northeast Forestry University, Harbin 150040, China; Engineering Research Center of Forest Bio-preparation, Ministry of Education, Northeast Forestry University, Harbin 150040, China; Heilongjiang Provincial Key Laboratory of ecological utilization of Forestry-based active substances, Harbin 150040, China
[b] Department of Chemistry, Division of Science and Technology, University of Education, Lahore, Pakistan
[c] Hisun Pharmaceutical (Hangzhou) Co., Ltd. No1, Road, Xukou Town, Fuyang District, Hangzhou, 311404, China

ARTICLE INFO

Keywords:
Juglone
Back extraction
Magnetic solid phase extraction
Bubble column
Purification

ABSTRACT

Juglone was first preliminary purified by back extraction (BE) which also completed the sustainability of microemulsion as a solvent for extraction of juglone in *J. mandshurica* Maxim. branches. Then, magnetic solid phase extraction (MSPE) based on bubble column (BC) was proposed to further purify the juglone, GO/ND/Fe_3O_4 as adsorbent, which broke through the limitation that MSPE is only suitable for trace enrichment. Thus, a BE combined with MSPE based on BC (BE-MSPE/BC) technology to separate and purify juglone from *J. mandshurica* Maxim. was developed. Under the optimal conditions (optimal adsorption conditions: 0.5 h of adsorption time, 30 mg/mL of solid-liquid ratio, 5.5 of pH, 60 L/min of air flow; optimal desorption conditions: 0.4 h of desorption time, methanol of desorption agent, 100% of desorbent volume fraction, 8 of pH, 40 mg/mL of solid-liquid ratio, 80 L/min of air flow rate), the recovery yield and purity of juglone obtained by BE-MSPE/BC were 80.57% and 72.38%, respectively. BE-MSPE/BC, as a green separation and purification technology that can easily achieve large-scale and sustainable production, is expected to be an alternative method to separate and purify active components in biomass materials and products.

1. Introduction

Juglans mandshurica Maxim. (*J. mandshurica* Maxim.), deciduous tree, commonly called the Manchurian walnut belongs to the Juglandaceae family. It is widely distributed in East Asia, Southeastern Europe, Oceania, North America and South America [1,2]. Previous studies on *J. mandshurica* Maxim. have shown that the plant is rich in active ingredients such as phenols, flavonoids, tetralones and naphthoquinones [3]. Quinones, including anthraquinone and naphthoquinones, are the main active ingredients in *J. mandshurica* Maxim. [4,5]. Juglone, the main quinone in *J. mandshurica* Maxim., has a wide range of biological activities and has been used in many fields. Juglone, known as a "natural pigment" and, is often used as a colorant in the printing and dyeing industry [6]. In agriculture, juglone is commonly used in pesticides and herbicides [7,8]. In addition, juglone has anti-diabetic, antibacterial, anti-inflammatory, anti-oxidant, anti-tumor activities and regulates intestinal flora, and therefore is often used in medicinal applications [9–12].

*Abbreviations: J. mandshurica*Maxim., *Juglans mandshurica*Maxim.; BE, back extraction; MSPE, magnetic solid phase extraction; BC, bubble column; BE-MSPE/BC, BE combined with MSPE based on BC; GO/ND/Fe_3O_4, graphene oxide/nano diamonds/Fe_3O_4; RMM-MAE, reverse micellar microemulsion-microwave assisted extraction; RMM, reverse micellar microemulsion; SEM, scanning electron microscope; XRD, X-ray diffraction; MSPE/BC, MSPE based on BC; MSPE/SA, shaker assisted MSPE; MSPE/VA, vortex assisted MSPE.

* Corresponding Author, Dr. Chunying Li; Dr. Chunjian Zhao, Key Laboratory of Forest Plant Ecology, Ministry of Education, Northeast Forestry University, Harbin 150040, China; College of Chemistry, Chemical Engineering and Resource Utilization, Northeast Forestry University, Harbin 150040, China; Engineering Research Center of Forest Bio-preparation, Ministry of Education, Northeast Forestry University, Harbin 150040, China; Heilongjiang Provincial Key Laboratory of ecological utilization of Forestry-based active substances, Harbin 150040, China. Tel./Fax: +86-451-8219-1387 (Chunying Li); +86-451-8219-0848

E-mail addresses: lcy@nefu.edu.cn (C. Li), zcj@nefu.edu.cn (C. Zhao).

https://doi.org/10.1016/j.cep.2022.109257
Received 16 September 2022; Received in revised form 24 November 2022; Accepted 18 December 2022
Available online 20 December 2022

Pruning is an indispensable technique to ensure healthy growth of *J. mandshurica* Maxim.. The branches from pruning are often discarded. Studies have shown that juglone is contained in the branches of *J. mandshurica* Maxim. [13]. Utilization of this coproducts as a resource to obtain juglone should be investigated. High-purity juglone is often obtained by time-consuming and high-cost technologies, such as chromatographic column method and semi-preparative chromatography [14–17]. This not only limits the recovery yield of juglone, but also results in the generation of a large amount of polluting waste during the purification process. Therefore, an efficient, sustainable and environmentally friendly method for separation and purification juglone is required.

Due to the drawbacks of traditional extraction solvents, such as high toxicity, high risk of environmental pollution during operation, low extraction yield, high cost, complex preparation and use procedures, non-recycling, and detection obstacles, the development of solvents for natural products extraction is on the rise [18]. Microemulsion is a new type of efficient and highly selective extraction solvent used in natural product extraction in recent years [19–22]. Compared with other solvents, greater interface area, higher selectivity, and higher solubility of compounds are advantages of microemulsion [23–25]. Nanoscale particle size of microemulsions yield a larger specific surface area than traditional solvents, which enables the target components to contact the microemulsion more fully [26]. However, the organic matrix of microemulsion limits the subsequent purification of natural products [27]. The introduction of back extraction (BE) can affect the interaction between the target components and the organic matrix in the microemulsion. The influence of salt concentration on the extraction yield of target components is mainly determined by the shielding effect of ions on the inner surface of reverse micelles. Dissociated counter ions in the main water phase can penetrate deep into the interface of the reverse micellar microemulsion (RMM) to form a potential difference, thereby generating an electromotive force. A lower salt concentration is conducive to solubilize of target components in the system. As the salt concentration increases, excess free ions will come between the "pool" and the oil phase of the RMM system. This will create an electrical double layer near the surfactant polar head groups. The adsorption interface produces an electrostatic shielding effect, which reduces the electrostatic force between target components and the adsorption interface and reduces the solubility of target components in the microemulsion system. Because of electrostatic shielding, the electrical double layer on the inner surface of the microemulsion becomes thinner, which further weakens the repulsive force of the surfactant polar groups. The reverse micelles then shrink. These factors clearly reduce the solubility of target components molecules in the microemulsion system and promote BE of target components. BE not only eliminates the influence of microemulsion organic matrix on the subsequent purification of the target component, but also it is the preliminary purification of the target component [28]. At the same time, the recovery and utilization of the microemulsion can be completed by BE.

Magnetic solid phase extraction (MSPE) has been widely used in the field of separation and enrichment due to its high efficiency, convenient recovery, without packing column and pretreatment of fillers, etc. [29–31]. The diffusion and mass transfer rate of MSPE are limited because of the disadvantages of auxiliary means used for MSPE (such as shaker). Which makes it currently only suitable for trace enrichment, such as sewage treatment, pretreatment for detection of pesticide residues in food and drug residues in blood samples, etc. [32,33]. The bubble column (BC) device previously developed by our research group can enhance the turbulence and mass transfer of the solid-liquid system in the bubble column by virtue of the bubbles continuously pumped into the suspension from the gas distributor at the bottom of the device [34]. In view of this, to make the application of MSPE achieve a breakthrough from trace enrichment to natural product purification, MSPE based on bubble column (MSPE/BC) was developed. Additionally, as a kind of emerging adsorbents, graphene oxide/nano diamonds/Fe_3O_4 (GO/ND/Fe_3O_4) with the advantages of high specific surface area, stable properties, low interlayer irreversible aggregation rate, and high active site exposure rate has been used in MSPE for target ingredient enrichment [35–39]. GO/ND/Fe_3O_4 can be used as adsorbent to adsorb and purify juglone for the following reasons. The juglone can be adsorbed and purified by the modified GO because of binding forces [40]. First, modification of GO with ND stops irreversible aggregation of GO sheets caused by strong van der Waals forces. This maximizes the number of exposed active sites and specific surface area of GO, and improves the adsorption capacity for purification of juglone by GO/ND/Fe_3O_4 [29, 40]. Second, the double hydrogen bond effect between GO and juglone molecules plays an important role in the adsorption and purification of GO. The quinone carbonyl group in juglone and the oxygen in the phenol hydroxyl group can form intermolecular hydrogen bonds with the hydroxyl hydrogen and carboxyl hydrogen in GO. In addition, the hydrogen in the phenol hydroxyl group of juglone quinone can also form intermolecular hydrogen bonds with the ether group oxygen, alcohol hydroxyl group oxygen and carboxyl group oxygen in GO. A π-hydrogen bond (i.e., aromatic hydrogen bond) also forms between juglone and GO. The large π-bond system of the benzene ring in the juglone quinone or GO structure has a large electron cloud density, which can act as a proton acceptor to form π-hydrogen bonds with oxygen atoms and hydrogen atoms connected to oxygen atoms. In addition to the hydrogen bonding between GO and juglone molecules, there is a coordination effect between the GO and juglone molecules. The carbonyl oxygen of juglone provides an empty orbit to form a coordinate bond with the ether oxygen and hydroxyl oxygen containing a lone pair of electrons in GO. If there is a double bond in the carbon adjacent to the hydroxyl oxygen that forms a hydrogen bond with the juglone carbonyl oxygen, the existence of this coordination bond will establish a p-π conjugation between juglone and GO, which will lengthen the conjugated chain of juglone. This will further strengthen the attraction and binding force of the hydroxyl and carbonyl groups in juglone, and improve the selectivity of GO for juglone. The phenol hydroxyl oxygen with a lone pair of electrons in juglone can also coordinate with the carboxyl-carbonyl oxygen containing empty orbitals in GO. This can also produce p-π conjugation, enhancing the absorption force and selective combination between GO and juglone molecules.

Considering the superiority of BE and MSPE/BC with GO/ND/Fe_3O_4 as adsorbents, BE combined with MSPE/BC (BE-MSPE/BC) technology was developed for purification of juglone from the co-products of *J. mandshurica* Maxim. The preliminary purification of juglone by back extraction lays the foundation for its further purification. The first combination of BC and MSPE provides the possibility for MSPE to break through the limitations of trace enrichment. Moreover, adjustability of bubble column volume, ease of operation and high efficiency of extraction and purification make BE-MSPE/BC suitable for large-scale production.

2. Materials and methods

2.1. Materials and chemicals

Branches of *J. mandshurica* Maxim. with knot-shaped longitudinal stripes, round protuberant stomata and triangular leaf mark were collected in November 2019 from the Maoershan Forest Test Station in China. The photo of *J. mandshurica* Maxim. branches was shown in Fig. S1. 1 kg branches with 37.28 % water content is transferred to 40 °C dryer (DGX-9073, Shanghai Fuma Experimental Equipment Co., Ltd, Shanghai, China) for 72 h after being dried in the shade [40]. Then they were crushed into 60 mesh of powder by grinder (YR-2500A, Yongkang Wurui Industry and Trade Co., Ltd, Jinhua, China).

Juglone standard (purity $\geq$ 98.0%) was purchased from Aladdin Chemistry (Shanghai, China). Acetonitrile (HPLC), phosphoric acid (HPLC) and other reagents (AR) were purchased from Fuchen Chemical Regents Factory (Shanghai, China).

2.2. Determination of juglone

High performance liquid chromatography (HPLC, Agilent 1260 Infinity, Santa Clara, CA, USA) was used for determination of juglone using a Diamonsil C_{18} column (4.6 mm× 250 nm, 5 μm; Dikma, Beijing). The mobile phase was a mixture of 0.2 % phosphoric acid aqueous solution (A) and pure methanol (B) in a ratio of 1:1 (v/v). Injection volume was 20 μl and flow rate was 1.0 mL/min [41].

2.3. Preliminary separation and purification of juglone by BE

The juglone contained in the *J. mandshurica* Maxim. branches was extracted by method of reverse micellar microemulsion-microwave assisted extraction (RMM-MAE) according to the conditions previously optimized by our research group [41]. After extraction, the RMM containing juglone was subjected to BE. The BE conditions were KCl solution and RMM at a ratio of 3:1 (V: V), KCl concentration of 2.0 mol/L, pH of 9.0, bubble column running time of 30 min, and air flow rate of 80 L/min. The mixed solution was left to stand in the bubble column until the layers were separated, indicating that the BE was completed. Take the upper layer solution to adjust the pH to 3.0 with HCl, the color change of the solution was observed.

The dehydrated microemulsion phase of the lower layer is released from the bottom of the bubble column and collected. Under magnetic stirring, 0.05 mol/L KCl solution was added dropwise to recover the RMM according to the ratio of 27:13.5:4.5:55 (Tween 80: n-propanol: n-hexane: 0.05 mol/L KCl, w: w: w: w).

2.4. Further separation and purification of juglone by MSPE/BC

2.4.1. Preparation and characterization of GO/ND/Fe_3O_4

GO/ND/Fe_3O_4 was prepared according to references [42,43] and characterized by Raman scattering, scanning electron microscope (SEM) and X-ray diffraction (XRD).

2.4.2. Purification procedure for juglone by MSPE/BC

The MSPE/BC of juglone was carried out in a bubble column device which is consisted of glass cylindrical container (ø 3 cm×14 cm), air inlet, sampling entrance, flow meter and pump (Fig. 1). The air flow of bubble column is controlled by a valve and measured by a flow meter [34]. Schematic diagram of bubble column device is shown in Fig. 1. GO/ND/Fe_3O_4 used as the adsorbent in MSPE/BC and the preliminary purified juglone obtained from the BE were added to the bubble column through the sampling entrance. The uniformity of suspension is maintained by accelerating mass transfer to improve the adequacy of solid-liquid contact through bubble turbulence.

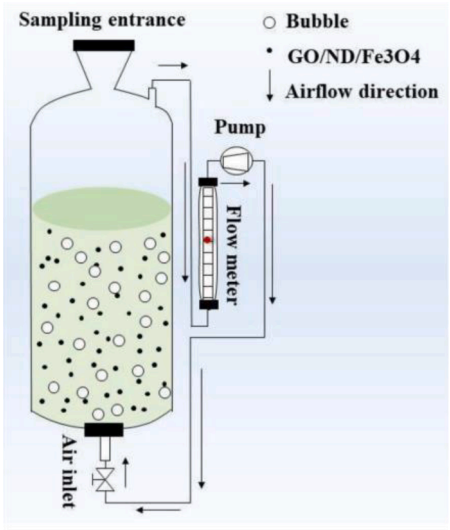

Fig. 1. Schematic diagram of adsorption or desorption process in MSPE/BC.

MSPE/BC is consisted of two processes: adsorption of juglone on GO/ND/Fe_3O_4 and desorption. GO/ND/Fe_3O_4 and the back extraction solution containing juglone were added to the bubble column then fully adsorbed for a certain time while maintaining a certain air flow to complete the MSPE/BC adsorption process. After the adsorption tests, the extract was separated from GO/ND/Fe_3O_4 by neodymium magnet. The neodymium magnet was placed on one side of bubble column, and GO/ND/Fe_3O_4 was enriched to this side by magnetic force for solid-liquid separation. After adsorption, the separated GO/ND/Fe_3O_4 was washed with deionized water at a solid-liquid ratio ($m_{GO/ND/Fe3O4}$ / V_{water}, mg/mL) of 10 to remove the residual BE solution on surface of GO/ND/Fe_3O_4. Desorbent was added to the bubble column containing GO/ND/Fe_3O_4. Subsequently, the desorbent in the bubble column and GO/ND/Fe_3O_4 loaded with juglone were kept for a certain period of time at a certain air flow rate to complete the MSPE/BC desorption process. After desorption was completed, GO/ND/Fe_3O_4 was separated from the desorption solution with the aid of neodymium magnet. Thus, the MSPE/BC process was completed. The adsorption yield (Y_a, %) and desorption yield (Y_d, %) of juglone were calculated using Eq. (1) and (2), respectively.

$$Y_a(\%) = \frac{(C_0 - C_a)V_a}{C_0\ V_a} \times 100 \quad (1)$$

$$Y_d(\%) = \frac{C_d V_d}{(C_0 - C_a)V_a} \times 100 \quad (2)$$

Where C_0 (mg/mL) and C_a (mg/mL) represent the concentrations of juglone in the extract before and after adsorption, respectively; V_a (mL) means the volume of the adsorption solution; C_d (mg/mL) represents the concentration of juglone in the desorption solution; and V_d (mL) means the volume of desorption solution.

2.4.3. Optimization of MSPE/BC process

2.4.3.1. Adsorption optimization of juglone on GO/ND/Fe_3O_4. The adsorption of juglone on GO/ND/Fe_3O_4 by MSPE/BC was optimized. Through adsorption kinetic tests and a series of single factor tests (solid-liquid ratio, pH and air flow rate) (Table 1), the best parameters of each factor were obtained. In the adsorption kinetics test, samples were collected once every 0.1 h. The adsorption yields (Y_a, %) of juglone on GO/ND/Fe_3O_4 were calculated using Eq. (1).

2.4.3.2 Desorption optimization of juglone on GO/ND/Fe_3O_4. The desorption of juglone on GO/ND/Fe_3O_4 by MSPE/BC was optimized. The factors affecting the desorption yield of juglone were explored by desorption kinetics test and single factor tests (type of desorbent, concentration of desorbent, pH, rate of air flow, solid-liquid ratio). In the desorption kinetics test, samples were collected once every 0.1h. The testing parameters are seen in Table 2. The desorption yields (Y_d, %) of

Table 1
Optimization of static adsorption conditions for juglone on GO/ND/Fe_3O_4.

Adsorption test conditions	Solid-liquid ratio ($m_{GO/ND/Fe3O4}$ / $V_{back\ extraction\ solution}$) (mg/mL)	pH	Rate of air flow (L/min)	Adsorption time (h)
Adsorption kinetics test	20	7	60	collected once every 0.1 h
Solid-liquid ratio optimization	10, 20, 30, 40, 50	7	60	0.5
pH optimization	20	4, 5.5, 7, 8.5, 10	60	0.5
Rate of air flow optimization	20	7	20, 40, 60, 80, 100	0.5

Table 2
Optimization of static desorption conditions for juglone on GO/ND/Fe_3O_4.

Desorption test conditions	Solid-liquid ratio ($m_{GO/ND/Fe3O4}$ / $V_{desorbent}$) (mg/mL)	pH	Rate of air flow (L/min)	Desorption time (h)	Desorbent types	Desorbent concentration (%)
Desorption kinetics test	30	7	60	collected once every 0.1 h	ethanol	100
Desorbent types optimization	30	7	60	0.4	ethanol, methanol, n-butanol	100
Desorbent concentration optimization	30	7	60	0.4	ethanol	60, 70, 80, 90, 100
Solid-liquid ratio optimization	10, 20, 30, 40, 50	7	60	0.4	ethanol	100
pH optimization	30	4, 6, 8, 10, 12	60	0.4	ethanol	100
Rate of air flow optimization	30	7	20,40,60,80,100	0.4	ethanol	100

juglone on GO/ND/Fe_3O_4 are calculated using Eq. (2).

2.4.4. Reusability of GO/ND/Fe_3O_4

Reusability of GO/ND/Fe_3O_4 was evaluated by repeating the adsorption and desorption process. After each desorption, the GO/ND/Fe_3O_4 was ultrasonically washed with water and ethanol at a solid-liquid ratio ($m_{GO/ND/Fe3O4}$ /$V_{water\ or\ ethanol}$, mg/mL) of 10 for 10 min, respectively. After drying the recovered GO/ND/Fe_3O_4 at 80°C for 2 h, it was then used in the next cycle [42].

2.4.5. Comparison of different methods

Vortex and shaker are the most commonly used auxiliary techniques in combination with MSPE [42–44]. The effects of shaker assisted MSPE (MSPE/SA) and vortex assisted MSPE (MSPE/VA) on juglone purification were compared with those of MSPE/BC. The adsorption yield (Y_a, %) and desorption yield (Y_d, %) of juglone were calculated using Eq. (1) and (2), respectively.

2.4.5.1 Juglone purification by MSPE/BC. GO/ND/Fe_3O_4 was added to a bubble column containing 35 L of back extract solution at a ratio of 30 mg/mL (GO/ND/Fe_3O_4: back extract, m:V). Then N2 was pumped into the bubble column at a rate of 60 L/min for 0.5 h to complete the adsorption of juglone. Subsequently, absolute ethanol was added at a ratio of 40 mg/mL (GO/ND/Fe_3O_4: absolute ethanol, m:V), and N_2 was promoted at a rate of 80 L/min for 0.4 h to complete the desorption of juglone.

2.4.5.2 Juglone purification by MSPE/SA. GO/ND/Fe_3O_4 was mixed with 250 mL back extract at a ratio of 30 mg/mL (GO/ND/Fe_3O_4: back extract, m:V) and shaken at a rate of 180 r/min for 24 h. After adsorption, absolute ethanol was added at a ratio of 40 mg/mL (GO/ND/Fe_3O_4: absolute ethanol, m:V) and shaken at 180 r/min for 24 h to desorb the juglone from GO/ND/Fe_3O_4.

2.4.5.3. Juglone purification by MSPE/VA. 30 mL of back extract was mixed with GO/ND/Fe_3O_4 at a ratio of 30 mg/mL (GO/ND/Fe_3O_4: back extract, m:V) in a centrifuge tube and vortexed for 0.5 h. Then, absolute ethanol was added to the GO/ND/Fe_3O_4 with juglone adsorbed at a ratio of 40 mg/mL (GO/ND/Fe_3O_4: absolute ethanol, m:V), and desorbed by 0.4 h vortexing.

2.5. Separation and purification of juglone by BE-MSPE/BC

After extraction by RMM-MAE, juglone was preliminarily purified by BE. The BE solution loaded with juglone was adsorbed and desorbed under the optimized conditions obtain from Section 2.4.3 to complete the MSPE/BC of juglone. Then desorption solution obtained from MSPE/BC was dried at 40°C using a rotary evaporator (RE-52AA, Shanghai QingPu Huxi Instrument Factory) to obtain purified juglone. The

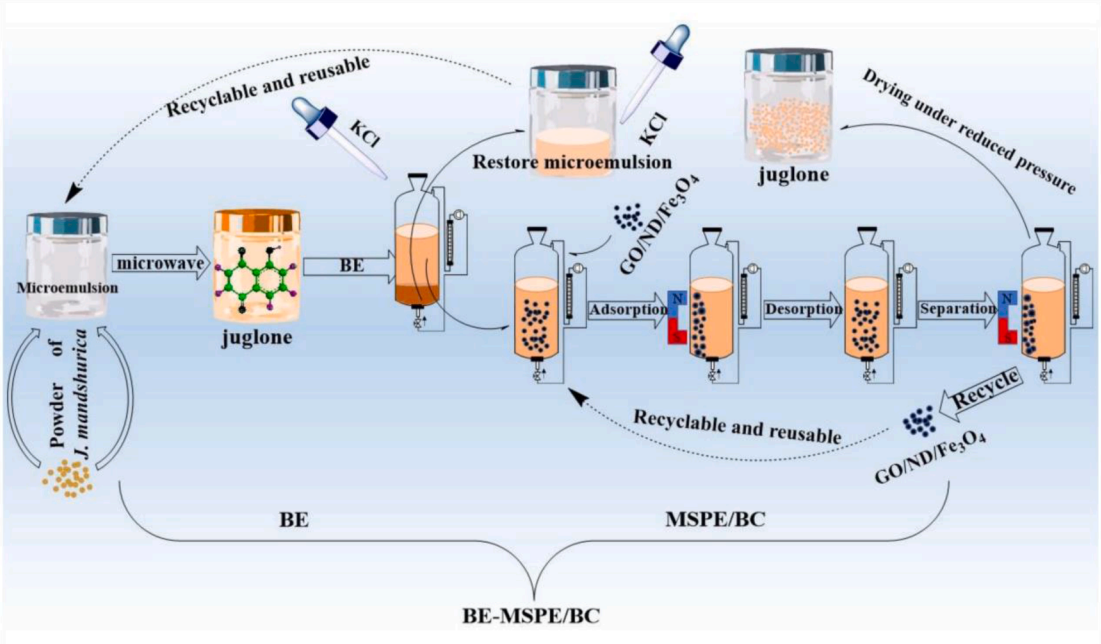

Fig. 2. The diagram of BE-MSPE/BC.

recovery yield and purity of juglone were calculated using Eqs. (3) and (4), respectively [45]. The diagram of BE-MSPE/BC was shown in Fig. 2.

$$R = \frac{C_d \times V_d}{C_e \times V_e} \times 100 \quad (3)$$

$$P = \frac{C_d \times V_d}{m_d} \times 100 \quad (4)$$

Where R (%) represent the recovery yield of juglone; C_d (mg/mL) represents the concentration of juglone in the desorption solution; V_d (mL) means the volume of desorption solution; *Ce* (mg/mL) represents the concentration of juglone in the extract; and *Ve* (mL) means the volume of extract. Where *P*(%) represents the purified purity of purified juglone; m_d (mg) is the mass of the powder obtained after the desorption liquid was spin-dried.

2.6. Statistic analysis

All the experiments were carried out in triplicates. Results were reported as a mean of triplicates with standard deviation (mean ± SD) or error bars in the graphs. Graphs were drawn using Origin 2021.

3. Results and discussion

3.1. Preliminary separation and purification of juglone by BE

Fig. S2B-a is the image of microemulsion extract enriched with juglone. The image of alkaline back extract is shown in Fig. S2A. Take the upper layer of back extract and it can be seen that it is purple-red (Fig. S2B-b), adjust its pH to 3 and the color will turn to orange (Fig. S2B-c). Which is consistent with the characteristic that juglone is purple-red in acidic solution and orange in alkaline solution. It indicates that juglone is successfully back extracted from the microemulsion into KCl aqueous solution.

3.2. Further separation and purification of juglone by MSPE/BC

3.2.1. Characterization of the GO/ND/Fe_3O_4

The characterizations of GO/ND/Fe_3O_4 are shown in Fig. 3. In the Raman spectrum, D band reflects the SP^3 hybridization of C atom, and G band indicates the SP^2 hybridization of the C atom. The ratio of I(D)/I(G) reflects the hybridization of C atom in the prepared materials (GO/ND/Fe_3O_4). It can be seen from Fig. 3A the I(D)/I(G) of GO/ND was 0.99 which was higher than that 0.82 of GO. Which indicated that SP^3 hybridization of GO/ND was enhanced, that was, its three-dimensional structure enhanced. Which implied that the ND of the regular tetrahedron structure had been successfully introduced into GO. The introduction of Fe_3O_4 further increased the I(D)/I(G) ratio of GO/ND/Fe_3O_4 to 1.40. It can be seen from the IR spectrum in Fig. 3B that the composite material, GO/ND/Fe_3O_4 contains hydroxyl groups, which can be indicated by the absorption peak near 3000 cm^{-1}. The carboxyl group is one of the functional groups of GO/ND/ND/Fe_3O_4, and its C=O characteristic stretching vibration appears at 1734 cm^{-1}. The absorption peak at 869 cm^{-1} just verified the existence of epoxy groups. In addition, the peak near 580 cm^{-1} corresponds to the existence of Fe-O bond, which proves the successful introduction of magnetic particles. The state of the spherical particles in Fig. 3C shows the uniform embedding of Fe_3O_4 particles on the GO surface [43]. According to the relevant peak information of XRD shown in Fig. 3D, the JCPDS card number is indexed, 89-8493 corresponds to the existence of ND. This is consistent with the results reported, which suggests that the increase of GO active sites for absorbing juglone may due to the existence of ND's supporting effect on GO sheets [42].

3.2.2. Optimization of the adsorption of juglone on GO/ND/Fe_3O_4

3.2.2.1 Adsorption kinetics. The adsorption yield of juglone gradually increased from 0 to 0.5 h and then remained relatively stable (Fig. 4A). After 0.5 h, the magnetic material may have become saturated so that no more juglone could be adsorbed. Therefore, 0.5 h was selected as the optimum adsorption time for subsequent experiments.

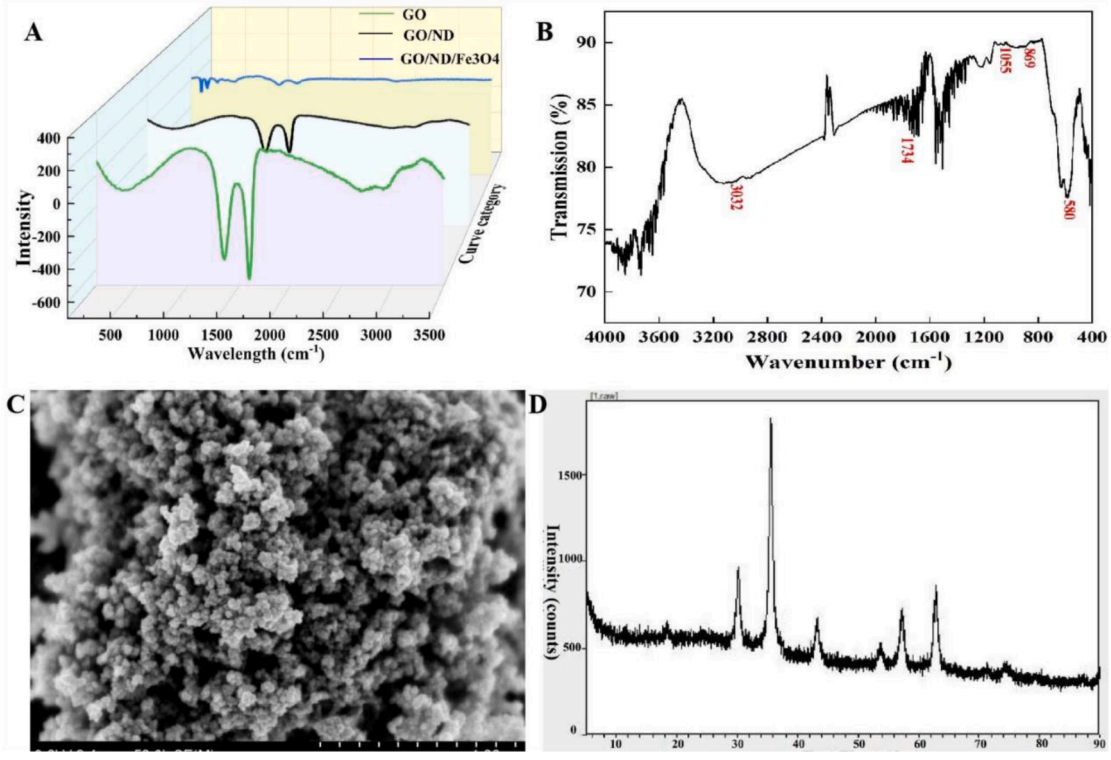

Fig. 3. Characterization of GO/ND/Fe_3O_4. A: Raman spectra of GO, GO/ND and GO/ND/Fe_3O_4. B: FTIR spectrum of GO/ND/Fe_3O_4. C: SEM image of GO/ND/Fe_3O_4, D: XRD image of GO/ND/Fe_3O_4.

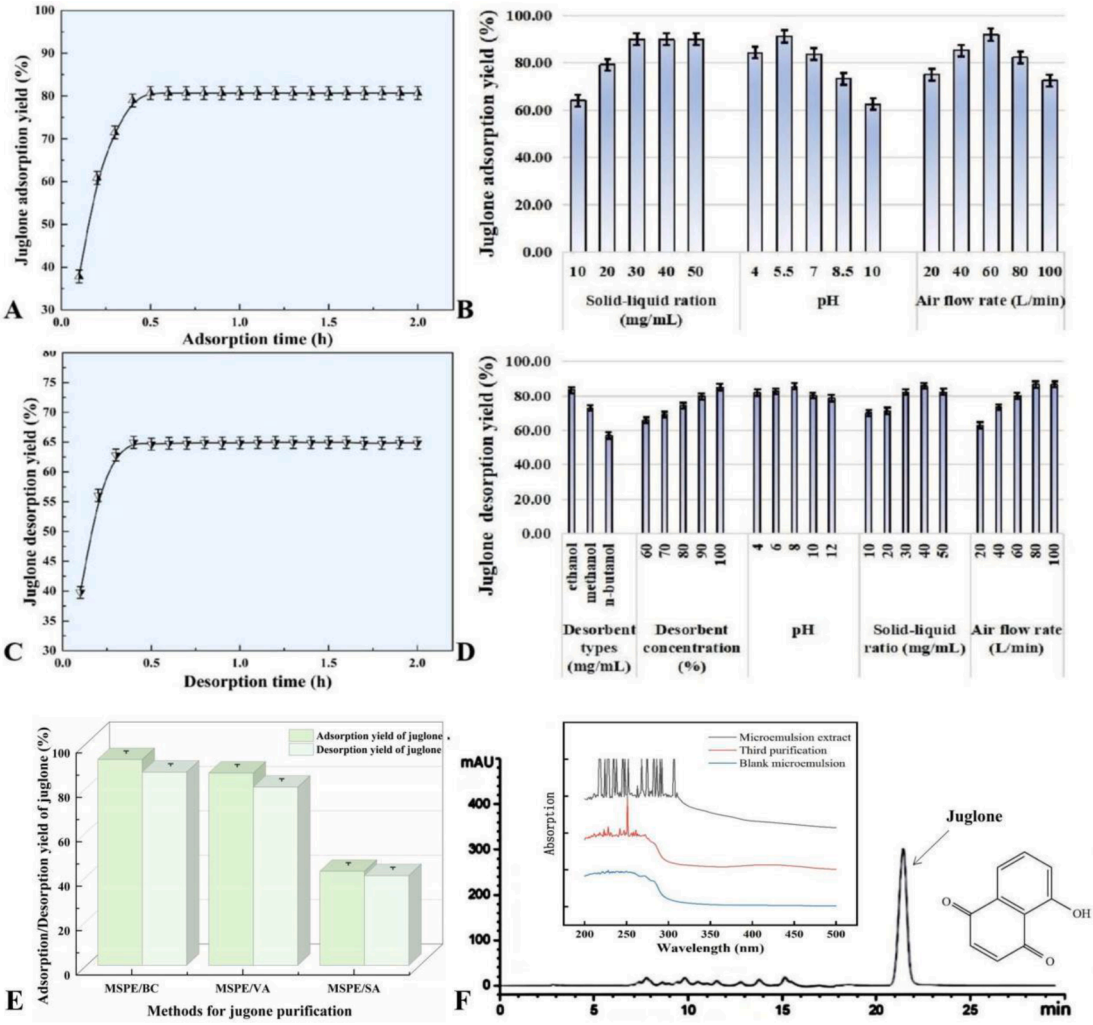

Fig. 4. Adsorption kinetic curve for juglone (A). Effect of single factors on the adsorption yield for juglone (B). Desorption kinetic curve for juglone (C). Effect of single factors on the desorption yield for juglone (D). Effects of different methods on adsorption and desorption yields of juglone (E). Purification results for juglone. A: HPLC spectrum of the purified juglone; B: Ultraviolet–visible spectrum of the sample (F).

3.2.2.2 Effect of solid-liquid ratio on the adsorption yield of juglone. Effect of solid-liquid ratio (10–50 mg/mL) on the adsorption yield of juglone on GO/ND/Fe_3O_4 was investigated (Fig. 4B). As the GO/ND/Fe_3O_4 concentration increased from 10 to 40 mg/mL, the adsorption of juglone gradually increased. When the GO/ND/Fe_3O_4 concentration was more than 40 mg/mL, the adsorption of juglone did not increase as further increases in the solid-liquid ratio. Both 30 mg/mL and 40 mg/mL GO/ND/Fe_3O_4 gave similar results, and therefore, to reduce costs, 30 mg/mL was selected as the optimum GO/ND/Fe_3O_4 concentration. Juglone was mainly adsorbed through interaction with the surface of the GO/ND/Fe_3O_4. When the solid-liquid ratio was less than 30 mg/mL, juglone in the sample solution was not completely adsorbed by GO/ND/Fe_3O_4. This was why the adsorption of juglone increased with increase of GO/ND/Fe_3O_4 ratio. When the solid-liquid ratio reached 30 mg/mL, the juglone was almost all absorbed onto GO/ND/Fe_3O_4. Therefore, further increased in the concentration of GO/ND/Fe_3O_4 did not increase the adsorption of juglone. This is consistent with the results reported in publication [46].

3.2.2.3. Effect of pH on the adsorption of juglone. The pH determines form of the juglone and type of charge on surface of GO/ND/Fe_3O_4, which in turn affects the adsorption of juglone on GO/ND/Fe_3O_4 [42]. We investigated the adsorption of juglone on GO/ND/Fe_3O_4 from pH 4-10.

With increases in the pH from 4 to 5.5, the adsorption of juglone on GO/ND/Fe_3O_4 gradually increased (Fig. 4B). The maximum adsorption occurred at pH 5.5. At pH values above 5.5, the adsorption of juglone on GO/ND/Fe_3O_4 was negatively correlated with the pH. GO contains carboxyl and phenol hydroxyl groups, and ionization of these groups will increase with increasing pH. As pH changes from acidic to alkaline, the negative charge of GO will gradually increase. Ionization of juglone followed the same trend as the carboxyl and phenol hydroxyl groups in GO, and degree of ionization increased with increases in the pH. When pH exceeded 5.5, the negative charges of both juglone and GO gradually increased because of increases in the degree of ionization. When juglone and GO are negatively charged, there will be electrostatic repulsion between them, and this will increase with increases in the pH. Thus, the adsorption yield of juglone by GO/ND/Fe_3O_4 will gradually decrease as the pH increases. In the pH range of 4-5.5, the carboxyl groups in GO will be negatively charged, but the degree of ionization of juglone at pH 4 will be weaker than that at pH 5.5 [42]. Therefore, there will be stronger electrostatic repulsion between GO/ND/Fe_3O_4 and juglone at pH 5.5 than that at pH 4. At pH values lower than 5.5, some of the GO/ND/Fe_3O_4 might be destroyed by the acid, which would affect the adsorption yield of juglone. Therefore, pH 5.5 was selected as the optimum pH for the adsorption of juglone on GO/ND/Fe_3O_4.

3.2.2.4 Effect of air flow rate on adsorption yield. The effect of the air flow rate (20-100 L/min) on adsorption yield of juglone using GO/ND/Fe_3O_4 was investigated. With increases in the air flow rate from 20 to 60

L/min, the adsorption yield of juglone increased gradually until it reached a maximum at 60 L/min (Fig 4B). The adsorption yield of juglone then decreased with further increases in the air flow. When the air flow was less than 60 L/min, GO/ND/Fe_3O_4 was not well dispersed in the sample solution because the low air flow rate resulted in insufficient contact between GO/ND/Fe_3O_4 and juglone, and incomplete adsorption. When the air flow was more than 60 L/min, the juglone was more vigorously dispersed, and the time that it was in contact with GO/ND/Fe_3O_4 was too short, which decreased the adsorption yield of juglone. The adsorption capacity of GO/ND/Fe_3O_4 on juglone increases first and then tends to be stable with the increase of air flow. This trend is similar to the results in publication [34]. Therefore, 60 L/min was selected as the optimum air flow for subsequent test.

3.2.3. Optimization of static desorption of juglone on GO/ND/Fe_3O_4

3.2.3.1 Desorption kinetics. The desorption yield of juglone gradually increased from 0 to 0.4 h (Fig. 4C), and then remained stable after 0.4 h. This may be the diffusion of juglone loaded on GO/ND/Fe_3O_4 in absolute ethanol after 0.4 h has reached equilibrium, and the desorbable juglone from GO/ND/Fe_3O_4 has basically been released into absolute methanol. Therefore, 0.4 h was selected as the optimum desorption time.

3.2.3.2 Effect of desorbent type on desorption yield. The desorbent type is a key parameter that affects the desorption of juglone. The desorbent should be strong enough to remove juglone from the surface of GO/ND/Fe_3O_4 but not damage the GO/ND/Fe_3O_4 [42, 43].

Methanol, ethanol and n-butanol with a volume fraction of 100% were selected as candidate desorbents to explore the desorption yield of juglone from GO/ND/Fe_3O_4. The maximum desorption yield of juglone was obtained with methanol (Fig. 4D).

3.2.3.3 Effect of desorbent volume fraction on the desorption yield of juglone. To determine the optimum volume fraction of desorbent, 60% -100% methanol was used to desorb juglone from GO/ND/Fe_3O_4 (Fig. 4D). The desorption yield of juglone increased with increases in the volume fraction of methanol. According to the principle of similar phase solubility, juglone is more easily dissolved in 100% methanol due to its weak polar which is similar to the results reported [14]. Therefore, 100% methanol was selected as the optimum volume fraction for desorption of juglone from GO/ND/Fe_3O_4.

3.2.3.4 Effect of pH on the desorption yield of juglone. The effect of pH on desorption yield of juglone was explored (Fig. 4D). When pH was in the range of 4-8, the desorption yield of juglone was positively correlated with pH. When pH exceeded 8, desorption yield of juglone begun to decrease. As increased in the pH, the hydrogen ion concentration in the desorbent decreased, so the ionization inhibition rate of the desorbent on GO/ND/Fe_3O_4 and juglone decreased. The increase in ionization degree of GO/ND/Fe_3O_4 made the surface of GO/ND/Fe_3O_4 negatively charged [42]. The ionization of juglone made it exist in the form of juglone anion. The electrostatic repulsion between GO/ND/-Fe_3O_4 and juglone increased with the increase of the ionization degree, and the probability of juglone desorption from GO/ND/Fe_3O_4 also increased. When pH was in the range of 4-8, the desorption yield of juglone gradually increased. When pH was higher than 8, the increase in alkalinity also increased the probability of saponification reaction of juglone, which may be the reason for the decrease in juglone content. Therefore, 8 was the optimal pH of the desorbent for subsequent experiments.

3.2.3.5 Effect of solid-liquid ratio on the desorption of juglone. The effect of solid-liquid ratio from10 to 50 mg/mL was investigated (Fig. 4D). From 10 to 40 mg/mL, the desorption yield was positively correlated with solid-liquid ratio. Above 40 mg/mL, increases in the solid-liquid ratio did not greatly increase the desorption yield of juglone. When the solid-liquid ratio was less than 40 mg/mL, the amount of juglone loaded on the GO/ND/Fe_3O_4 was not enough to make the desorption solution saturate when it was desorbed. With an adsorbent concentration of 40 mg/mL, the desorption reached saturation and further increased the solid-liquid ratio (more than 40 mg/mL), the desorption yield of juglone did not increase.

3.2.3.6 Effect of air flow on the desorption of juglone. With increases in the air flow from 20 to 80 L/min, the desorption yield of juglone increased gradually until it reached a maximum at 80 L/min (Fig 4D). The adsorption yield of juglone then no longer increased significantly with further increases in the air flow. When the air flow rate was less than 80 L/min, juglone-loaded GO/ND/Fe_3O_4 did not well dispersed in the desorbent. Juglone loaded on GO/ND/Fe_3O_4 did not fully contact with the desorbent. With the increase of air flow, the dispersion of GO/ND/Fe_3O_4 in the desorbent increases, and the contact between juglone and the desorbent also increases, so the desorption rate of juglone gradually increases. When the air flow reaches 80 L/min, the contact between juglone and the desorbent is enough to make the juglone adsorbed on GO/ND/Fe_3O_4. Therefore, considering energy saving and efficiency, 80 L/min was determined as the optimal air flow rate.

3.2.4. Reusability

For recycling of GO/ND/Fe_3O_4, the reusability of magnetic composite materials was investigated and the results are shown in Table 3. After cycle 8, yield of the GO/ND/Fe_3O_4, adsorption yield, desorption yield, and purity of juglone are all relatively stable. However, after the 9^{th} recycling, although the GO/ND/Fe_3O_4 recovery yield did not decrease significantly, adsorption yield, desorption yield and purity of juglone all appeared to be greatly reduced. Therefore, GO/ND/Fe_3O_4 can be reused 9 times for the purification of juglone.

3.2.5. Comparison of different methods

MSPE/BC was compared with MSPE/SA and MSPE/VA for purification of juglone. It can be seen from Fig. 4E that the adsorption and desorption yields of juglone obtained through MSPE/BC were 2.19- and 2.15-fold higher than those obtained by MSPE/SA, respectively. While, MSPE/BC and VA/MASP were equivalent in terms of adsorption and desorption yields of juglone. It may be the reason that MSPE/SA cannot make adsorbent, GO/ND/Fe_3O_4, fully dispersed in liquid, and the aggregation of GO/ND/Fe_3O_4 limited the exposure rate of active sites. Which greatly reduces the ability to purify juglone by MSPE/SA. While, the turbulent flow and the continuous bottom-up bubbles induced by MSPE/VA and MSPE/BC, respectively, can promote the full desorption of GO/ND/Fe_3O_4 in the liquid. Thus, the adsorption and desorption capacity of GO/ND/Fe_3O_4 is maximized. Which makes it a possible for MSPC/BC to break through the limitation of MSPE on trace enrichment. Moreover, the volume of the back extract purified by MSPE/BC was 35000 mL, which was much larger than the volume of 250 mL purified by MSPE/SA and 30 mL by MSPE/VA. Therefore, MSPE/BC not only makes up for the deficiency that MSPE is generally only suitable for trace enrichment, but also endows MSPE with the potential for industrial production [46–48].

Table 3
Reuse of GO/ND/Fe_3O_4.

Cycles	Recovery rate of GO/ND/Fe_3O_4(%)	Adsorption yield of juglone (%)	Desorption yield of juglone (%)	Purity of Juglone (%)
0	99.76	70.30	50.60	70.86
1	99.75	70.22	50.31	70.22
2	99.70	69.95	50.04	69.03
3	99.67	69.97	49.20	68.90
4	99.61	69.71	49.02	68.11
5	99.52	69.42	48.63	67.56
6	99.50	68.50	47.81	64.30
7	99.46	66.36	45.25	62.47
8	99.40	63.14	41.96	60.89
9	99.33	51.80	34.46	48.61

3.3. Separation and purification of juglone by BE-MSPE/BC

The desorption solution obtained by MSPE/BC was analyzed by HPLC and ultraviolet–visible spectroscopy (Fig. 4F). The HPLC spectra of the purified juglone sample was shown in Fig. 7A. The purity and recovery yield of juglone obtained by BE-MSPE/BC were 72.38% and 80.57%, respectively.

4. Conclusions

The technology developed in this study, MSPE/BC, for the separation and purification of juglone from coproducts of *J. mandshurica* Maxim. is efficient and sustainable. Meanwhile, it solves the cumbersome problem of chromatographic column packing in traditional natural product purification methods. Furthermore, MSPE/BC makes up for the deficiency that MSPE is generally only suitable for trace enrichment and endows MSPE with the potential for industrial production. Consequently, the results of this study could be used as a guideline for the development of alternative technology for separation and purification active ingredients from biomass materials and products.

CRediT authorship contribution statement

Mengfei Tian: Conceptualization, Methodology, Writing – original draft. **Xianming Meng:** Validation, Investigation. **Naveed Ahmad:** Writing – review & editing. **Chunying Li:** Project administration, Writing – review & editing. **Zhanyu Yuan:** Supervision, Resources. **Zidan Luo:** Validation, Investigation, Data curation. **Yu Zhang:** Validation, Investigation, Data curation. **Chunyu Liang:** Methodology, Investigation, Data curation, Software. **Chunjian Zhao:** Supervision, Resources, Funding acquisition, Project administration.

Declaration of Competing Interest

No

Data Availability

Data will be made available on request.

Acknowledgments

This work was supported by the Fundamental Research Funds for the Central Universities (Project No. 2572022DP06), and the 111 Project of China (B20088).

Supplementary materials

Supplementary material associated with this article can be found, in the online version, at doi:10.1016/j.cep.2022.109257.

References

[1] L.L. Lou, Z.Y. Cheng, R. Guo, G.D. Yao, S.J. Song, Alkaloids from *Juglans Mandshurica* maxim induce distinctive cell death in hepatocellular carcinoma cells, Nat. Prod. Res. 33 (2017) 911–914, https://doi.org/10.1080/14786419.2017.1413571.

[2] F. Li, Y. Li, Z.P. Deng, X.J. Zhu, Z.G. Zhang, X.D. Zhang, J.L Tian, W. Li, P. Zhao, Traditional uses, phytochemistry, pharmacology and clinical applications of Cortex *Juglandis Mandshuricae*: A comprehensive review, J. Ethnopharmacol. 285 (2022), 114887.

[3] S. Piao, Y. Qi, M. Jin, S. Diao, W. Zhou, J. Sun, X. Jin, G. Li, Two new quinones and six additional metabolites with potential anti-inflammatory activities from the roots of *Juglans mandshurica*, Nat. Prod. Res. 36 (2021) 3396–3403.

[4] Y. Zhao, W. Zhou, S. Diao, Z. Jiang, M. Jin, G. Li, Phytochemical investigation on the roots of *Juglans mandshurica* and their chemotaxonomic significance, Bionchem. Syst. Ecol. 87 (2019) 103957–103961.

[5] Y. Zhou, B. Yang, Y. Jiang, Z. Liu, Y. Liu, X. Wang, H. Kuang, Studies on Cytotoxic Activity against HepG-2 Cells of Naphthoquinones from Green Walnut Husks of *Juglans mandshurica* Maxim, Molecules 20 (2015) 15572–15588.

[6] J. Wizi, L. Wang, X. Hou, Y. Tao, B. Ma, Y. Yang, Ultrasound-microwave assisted extraction of natural colorants from sorghum husk with different solvents, Ind. Crop. Prod. 120 (2018) 203–213.

[7] Y. Akhtar, M.B. Isman, C.H. Lee, S.G. Lee, H.S. Lee, Toxicity of quinones against two-spotted spider mite and three species of aphids in laboratory and greenhouse conditions, Ind. Crop. Prod. 37 (2012) 536–541.

[8] X.F. Shang, Z.M. Zhao, J.C. Li, G.Z. Yang, J.Y. Zhang, Insecticidal and antifungal activities of *Rheum palmatum L.* anthraquinones and structurally related compounds, Ind. Crop. Prod. 137 (2019) 508–520.

[9] F. Gökalp, The chemical activity of Juglone in different phases as a protective agent, J. Fluor. Chem. 242 (2021), 109701.

[10] Y.T. Tang, Y. Li, P. Chu, X.D. Ma, Z.Y. Tang, Z.L. Sun, cancer therapies: Juglone and its derivatives, the future of development, Biomed, Pharmacother. 148 (2022), 112785.

[11] A. Seetha, H. Devaraj, G. Sudhandiran, Effects of combined treatment with Indomethacin and Juglone on AOM/DSS induced colon carcinogenesis in Balb/c mice: Roles of inflammation and apoptosis, Life Sci. 264 (2021), 118657.

[12] C. Shang, Y. Cao, C. Sun, Y. Li, Comparison of the excited-state proton transfer and single electron transfer mechanisms of the natural antioxidant Juglone and its dimer 3,3′-bijuglone, J. Photochem. Photobiol., A 427 (2022), 113825.

[13] S.N. Cosmulescu, T. Ion, A. Gheorghe, B. Mihai, G. Marius, Phenolics of Green Husk in Mature Walnut Fruits, Hort. Agrobot. Cluj. 38 (2010) 53–56.

[14] Y. Wang, X.Y. Chen, Y.X. Tian, S.J. Bai, G.M. She, Enriching technic-process of juglone-constituents from Qinglongyi, Int. J. Pharm. Res. 44 (2017) 60–64.

[15] L. Ma, L.Y. Zhang, J.Q. Han, X.Y. Zhou, S.S. Xia, Separation and purification of juglone from walnut green husk by macroporous resin, Food Ferment. Ind. 42 (2016) 108–113.

[16] J. Li, Z.Y. Qu, X. Zou, Y.B. Ji, lsolation and identification of juglone in pericarpium juglans, J. Harbin Univ. Commer., Nat. Sci. Ed. 27 (2011) 641–644.

[17] G.W. Luo, C.Q. Bai, H. Xiong, Q. Zhao, L. Lei, L.Q. Xu, J.F. Zhang, Z.Y. Hu, T. Fan, Comparison research on two methods for determining entrapment efficiency of Juglone liposome, Sci. Technol. Food Ind. 36 (2015) 146–150.

[18] F. Chemat, Z.E. Huma, M.K. Khan, Applications of ultrasound in food technology: Processing, preservation and extraction, Ultrason. Sonochem. 18 (2010) 813–835.

[19] D. Qin, B. Xiang, X. Zhou, S. Qiu, J. Xi, Microemulsion as solvent for naphthoquinones extraction from walnut (*Juglans mandshurica* Maxim) green husk using high voltage electrical discharge, Sep. Purif. Technol. 281 (2022), 119983.

[20] A. Sakdamas, K. Kongpol, S. Khongphan, F. Makkliang, W. Putalun, G. Yusakul, The hydrophobic deep eutectic solvents for extraction of curcuminoids and arturmerone from the *curcuma longa* L, Planta Med. 396 (2022), 133728.

[21] M. Jalali-Jivan, S. Abbasi, B. Fathi-Achachlouei, Lutein extraction by microemulsion technique: evaluation of stability versus thermal processing and environmental stresses, LWT–Food Sci. Technol. 16 (2021) 111839.

[22] N. Nan-Nkr, E. Aam, F. Altay, A. Akyldz, Extraction of carotenoid compounds from watermelon pulp with microemulsion based technique: optimization studies, Food Chem. 380 (2022), 132169.

[23] P. Szumaa, A. Macierzanka, Topical delivery of pharmaceutical and cosmetic macromolecules using microemulsion systems, Int. J. Pharm. 615 (2022), 121488.

[24] Y. Guo, H.Y. Li, Y.H. Yuan, J. Huang, J. Diao, B. Xie, Microemulsion extraction: An efficient way for simultaneous detoxification and resource recovery of hazardous wastewater containing V(V) and Cr(VI), J. Hazard. Mater. 386 (2020), 121948.

[25] X.C. Zhu, M. He, W. Zhang, H.B. Wei, X.J. Lyu, Q.B. Wang, X.F. You, L. Li, Formulation design of microemulsion collector based on gemini surfactant in coal flotation, J. Cleaner Prod. 257 (2020), 120496.

[26] D.Y. Qin, B. Xiang, X. Zhou, S.Y. Qiu, J. Xi, Microemulsion as solvent for naphthoquinones extraction from walnut (*Juglans mandshurica* Maxim) green husk using high voltage electrical discharge, Sep. Purif. Technol. 281 (2021), 119983.

[27] W.I. Mortada, M.M. El-Defrawy, E. Erfan, H.A. El-Asmy, Cloud point extraction coupled with back-extraction for speciation of inorganic vanadium in water and determination of total vanadium in food samples by ICP-OES, J. Food Compos. Anal. 108 (2022), 104445.

[28] D.S. Mathew, R.S. Juang, Improved back extraction of papain from AOT reverse micelles using alcohols and a counter-ionic surfactant, Biochem. Eng. J. 25 (2005) 219–225.

[29] L.A. Akamine, D.A. Vargas Medina, F.M. Lancas, Magnetic solid-phase extraction of gingerols in ginger containing products, Talanta 222 (2021), 121683.

[30] B. Feriduni, A. Mohebbi, M.A. Farajzadeh, M. Namvar, Magnetic graphene oxide–based solid-phase extraction combined with dispersive liquid–liquid microextraction for the simultaneous preconcentration of four typical pesticide residues in fruit juice and pulp, Food Anal. Methods 12 (2019) 2742–2752.

[31] Y. Li, S. Wang, Z. Xie, R. Xing, R. Wang, X. Chen, S. Hu, Deep eutectic solvent - loaded FeO@MIL-101(Cr) with core–shell structure for the magnetic solid phase extraction of non-steroidal anti-inflammatory drugs in environmental water samples$_{34}$, Microchem. J. 184 (2023), 108150.

[32] M.R. Bayatloo, S. Nojavan, Rapid and simple magnetic solid phase extraction of bisphenol a from bottled water, baby bottle, and urine samples using green magnetic hydroxyapatite/β-cyclodextrin polymer nanocomposite, Microchem. J. 175 (2022), 107180.

[33] L. Chen, B. Chen, Z. Zhou, Y. Liang, Z. Wu, M. He, B. Hu, Covalent organic framework-based magnetic solid phase extraction coupled with micellar electrokinetic chromatography for the analysis of trace organophosphorus pesticides in environmental water and atmospheric particulates, J. Chromatogr. A 1673 (2022), 463030.

[34] C.J. Zhao, Y.G. Zu, C.Y. Li, Extraction of solanesol from tobacco (*Nicotiana tobaccum* L.) leaves by bubble column, Chem. Eng. Process 48 (2009) 203–208.
[35] Q. Sheng, J. Li, Y. Chen, X. Liang, M. Lan, Hydrophilic graphene oxide-dopamine-cationic cellulose composites and their applications in N-Glycopeptides enrichment, Talanta 226 (2021) 122112–122119.
[36] Y. Dou, Q. Bai, W. Guo, S. Chen, H. Wang, The influences of internal interactions and functional groups on the adsorption of graphene and graphene oxide with alumina substrate, Comput. Mater. Sci. 214 (2022), 111733.
[37] J. Deng, L. Xiao, S. Yuan, W. Wang, X. Zhan, Z.-H. Hu, Activation of peroxymonosulfate by CoFeNi layered double hydroxide/graphene oxide (LDH/GO) for the degradation of gatifloxacin, Sep. Purif. Technol. 255 (2021), 117685.
[38] B. Dąbrowski, A. Żuchowska, Z. Graphene oxide internalization into mammalian cells – a review, Colloids Surf., B 221 (2023), 112998.
[39] R. Zhao, X. Yang, M. Li, X. Peng, M. Wei, X. Zhang, L. Yang, J. Li, Biodiesel preparation from *Thlaspi arvense* L. seed oil utilizing a novel ionic liquid core-shell magnetic catalyst, Ind. Crops Prod. 162 (2021), 113316.
[40] C. Li, X. Meng, M. Tian, S. Li, C. Zhao, A novel method to extract juglone from *Juglans mandshurica* waste branches using a water-in-oil microemulsion, Waste Biomass Valorization 13 (2022) 1547–1563.
[41] M. Khan, E. Yilmaz, B. Sevinc, E. Sahmetlioglu, M. Soylak, Preparation and characterization of magnetic allylamine modified graphene oxide-poly(vinyl acetate-co-divinylbenzene) nanocomposite for vortex assisted magnetic solid phase extraction of some metal ions, Talanta 146 (2016) 130–137.
[42] E. Yilmaz, H.I. Ulusoy, O. Demir, M. Soylak, A new magnetic nanodiamond/graphene oxide hybrid (Fe3O4@ND@GO) material for pre-concentration and sensitive determination of sildenafil in alleged herbal aphrodisiacs by HPLC-DAD system, J. Chromatogr. B 1084 (2018) 113–121.
[43] J.L. Zhao, P.F. Huang, X.M. Wang, J. Yang, Z. Zhou, X.Z. Du, X.Q. Lu, Efficient adsorption removal of organic nitrogen pesticides: Insight into a new hollow NiO/Co@C magnetic nanocomposites derived from metal-organic framework, Sep. Purif. Technol. 287 (2022), 120608.
[44] Z. Zhang, H.C. Schniepp, D.H. Adamson, Characterization of graphene oxide: Variations in reported approaches, Carbon 154 (2019) 510–521.
[45] M.F. Tian, C.Y. Liang, N. Ahmad, C.Y. Li, W.H. Wang, Y. Zhang, Z.D. Luo, L.Q. Qiu, C.J. Zhao, Proposal and application of a novel extraction and purification technology for juglone from *Juglans mandshurica* waste branches: Reverse micellar microemulsion combined with magnetic solid phase extraction, Chem. Eng. Res. Des. 186 (2022) 661–671, z.
[46] J. Liu, Z. Su, Q. Xu, Y. Shi, D. Wu, L. Li, Y. Wu, G. Li, Facile synthesis of boric acid-functionalized magnetic covalent organic frameworks and application to magnetic solid-phase extraction of trace endocrine disrupting compounds from meat samples, Food Chem. 399 (2023), 133843.
[47] B. Zhao, M. He, B. Chen, B. Hu, Facile green synthesis of magnetic porous organic polymers for fast preconcentration of trace lead and mercury from environmental water followed by graphite furnace atomic absorption spectrometry detectiont, Spectrochim. Acta, Part B 196 (2022), 106524.
[48] X.L. Song, H. Lv, K.C. Liao, D.D. Wang, G.M. Li, Y.Y. Wu, Q.Y. Chen, Y. Chen, Application of magnetic carbon nanotube composite nanospheres in magnetic solid-phase extraction of trace perfluoroalkyl substances from environmental water samples, Talanta 253 (2023), 123930.